c.3

LA-2035

CIC-14 REPORT COLLECTION
REPRODUCTION
COPY

LOS ALAMOS SCIENTIFIC LABORATORY
OF THE UNIVERSITY OF CALIFORNIA o LOS ALAMOS NEW MEXICO

A REVIEW OF THE CORROSION BEHAVIOR OF URANIUM

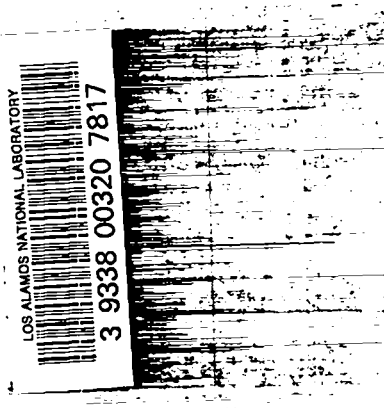

LEGAL NOTICE

This report was prepared as an account of Government sponsored work. Neither the United States, nor the Commission, nor any person acting on behalf of the Commission:

A. Makes any warranty or representation, express or implied, with respect to the accuracy, completeness, or usefulness of the information contained in this report, or that the use of any information, apparatus, method, or process disclosed in this report may not infringe privately owned rights; or

B. Assumes any liabilities with respect to the use of, or for damages resulting from the use of any information, apparatus, method, or process disclosed in this report.

As used in the above, "person acting on behalf of the Commission" includes any employee or contractor of the Commission to the extent that such employee or contractor prepares, handles or distributes, or provides access to, any information pursuant to his employment or contract with the Commission.

Printed in USA. Price $1.25. Available from the

Office of Technical Services
U. S. Department of Commerce
Washington 25, D. C.

LA-2035
METALLURGY AND CERAMICS
(TID-4500, 14th ed.)

LOS ALAMOS SCIENTIFIC LABORATORY
OF THE UNIVERSITY OF CALIFORNIA LOS ALAMOS NEW MEXICO

REPORT WRITTEN: April 1956

REPORT DISTRIBUTED: December 29, 1958

A REVIEW OF THE CORROSION BEHAVIOR OF URANIUM

By

James T. Waber

This report expresses the opinions of the author or authors and does not necessarily reflect the opinions or views of the Los Alamos Scientific Laboratory.

Contract W-7405-ENG. 36 with the U. S. Atomic Energy Commission

ABSTRACT

Unpublished work at this Laboratory on the corrosion of unalloyed uranium is summarized in this report. Data are presented for dry air and oxygen and for attack by water, water vapor, and steam, as well as by moist air and helium. The role of lattice defects in the corrosion mechanism is also discussed.

Particular attention has been given to the effects of impurities and test conditions on the rates of corrosion. The general inability to obtain reproducible data has been attributed to the influence of small obscure variations in the test procedure. The effects of intentional impurity additions appear to be small.

CONTENTS

TABLES

FIGURES

1. INTRODUCTION

In a number of ways, uranium is similar to iron in its corrosion behavior. For example, it is quite resistant in dry air or other atmospheres but, like iron, does corrode rapidly in the presence of moisture. Under conditions of differential aeration, the oxygen-depleted region on uranium becomes anodic, and it has been demonstrated that current will flow between immersed pieces of uranium supplied with different amounts of oxygen. Strong nitric acid attacks uranium only to a limited extent, although other acids readily dissolve it. The complete analogy with the passive behavior of iron in strong nitric acid has not been demonstrated. Although uranium and iron may behave similarly in these ways, the subject of uranium corrosion is complex and the difficulty of obtaining reproducible data in repeated experiments makes the experimental verification of any reaction mechanism quite difficult.

1.1 Storage of Uranium

Experience gained at Los Alamos in the storage of uranium strongly indicates that the best all-around atmosphere is freely circulating air and that attempts to enclose the metal or surround it with an inert gas only encourage greater corrosion.

In general, the metal can be handled with a minimum number of precautions and these are prescribed more by personnel health and safety requirements than by the pyrophoric character of the metal. It has been our casual experience that metal stored out of contact with air for several months develops corrosion products, presumably from reaction with moisture, which will ignite spontaneously in air at room temperature. The mechanism for forming these is not understood, but the behavior suggests the influence of uranium hydride.

The adherence of the corrosion products is favored by freely circulating air, whereas considerable spallation occurs under oxygen-starvation conditions. Relatively coherent sheets of corrosion products will, in some cases, detach themselves from the oxidizing metal. In a laboratory experiment using moist helium, eight distinct layers of oxide could be removed. The

oxide tends to be more voluminous in inert atmospheres, where there is restricted access of oxygen. We have observed porous oxide scales almost ten times as thick as the metal sheet from which they were formed. This formation occurred in a closed container in which there was also a considerable amount of water vapor.

On the basis of our experience and laboratory experiments, air or oxygen is preferable to an inert gas if there is any likelihood that moisture will be confined with the gas. All sources of moisture such as imperfect desiccants, damp containers, moist gas, etc., should be investigated and minimized. Our experience strongly indicates that circulating air is preferable to stagnant air.

1.2 Products Formed

Uranium dioxide, which has a face-centered-cubic fluorite lattice, is the major product formed in moist or dry air. In the vicinity of 185°C, higher oxides such as U_4O_9 or U_3O_8 become the principal products in the presence of water. The analysis of the products formed suggests that hydroxides, hydride, and higher hydrated oxides may also be present, depending on conditions.

The monoxide of uranium, UO, with the NaCl cubic lattice is usually found only in thin films on the metal, although it has occasionally been formed in laboratory experiments. It comprises the major product when uranium is heated in good vacua at temperatures higher than 600°C.

On the basis of electron-diffraction studies, the first oxide to be formed in vacuum at atmospheric temperatures is the dioxide, and no evidence for the monoxide has been obtained. This is contrary to some of our earlier findings.

2. THEORETICAL CONSIDERATIONS

The details of ionic as well as electronic motion across the film are an essential feature of a present-day discussion of the oxidation of metal. This is a reflection of the success of Wagner's and Schottky's concepts[1,2] of lattice defects in explaining most of the phenomena. Wagner[2] pointed out that oxidation of most metals could not proceed by diffusion if Dalton's law of ideal proportions held strictly true, but that it is the departure from stoichiometry which permits a diffusion gradient to exist across a compound scale.

The uranium-oxygen system has many distinguishable phases, which have been discussed by Gronvold,[3] Perio,[4] and others, and the composition range

of the "dioxide" is wide. However, it is not appropriate to discuss this literature critically in this report. Since uranium dioxide is the major constituent of most of the corrosion films, attention will be centered on the lattice defects and electrical conduction in this phase.

2.1 Type of Defects

The fluorite lattice of uranium dioxide can tolerate both excess anions and anion vacancies. In the region where the oxygen/uranium ratio is greater than 2, interstitial oxygen ions are distributed randomly among the several $(\frac{1}{2}, 0, 0)$ sites in the lattice. Perio[4] has observed a face-centered-cubic lattice of the approximate composition U_4O_9 (a ratio of 2.25). Hering and Perio[5] have also prepared face-centered-cubic compositions containing less than two oxygen atoms for each uranium atom.

Hund and his collaborators[6-9] have investigated the constitutional diagrams of rare-earth oxides with U_3O_8 and have observed solid solutions which retain the fluorite lattice from oxygen/metal ratios in excess of 2 down to 1.75. At any lower values of the ratio, the C-type rare-earth sesquioxide lattice (Mn_2O_3 type) is observed. This lattice is related to the fluorite lattice; the missing oxygens are ordered in the Mn_2O_3 structure. Comparison of the lattice parameters with the observed densities strongly indicates that anion vacancies predominate over interstitial cations for values of oxygen/metal ratios less than 2.00.

Rudorff and Valet,[10] Trzebiatowski and Selwood,[11] Slowinski and Elliott,[12] and Lambertson and Mueller,[13] have investigated the UO_2–ThO_2 phase diagram and found a continuous range of solid solutions. Hund and Niessen,[14] who worked with air-annealed specimens, found a two-phase region (fluorite + U_3O_8) above 60 mole % uranium oxide. The lattice parameter data are summarized in Fig. 1 and show excellent agreement among the four investigations where the solid solutions were annealed in hydrogen or vacuum. Hund and Niessen comment on the presence of U^{+6} and excess oxygen in their samples. Anderson et al.[15] studied the oxidation of these solid solutions and found no evidence for any type of defect other than interstitial anions. The proportion of cationic vacancies must be small in comparison.

The behavior may be discussed in terms of vacant anion sites and interstitial anions. The interchange of an oxygen atom between a given site in anion sub-lattice and an interstitial position such as envisaged in the Frenkel type of disorder can therefore be expected. Recent studies by Kurnick[16] on the mode of ionic conduction in AgBr, which is known to contain Frenkel defects, suggest that the transference number for interstitial Br^- ions is much larger than for the accompanying anion vacancies.

To date, no experiments on UO_2 have been performed, but the ease with

which excess oxygen is accommodated in the lattice with only slight shrinkage in lattice parameter strongly suggests that migration of interstitial anions might be only slightly impeded by the other oxygens. (See the data of Hund and Niessen in Fig. 1, which is compared with that of the other investigators.) The easy oxidation of UO_2 at low temperatures is in accord with the idea of low energy barriers.

2.2 Mode of Conduction

The fairly high electrical conductivity of UO_2 compacts suggests that it is a semiconductor. The conductivity is known to increase slightly with oxygen pressure. The Hall-effect experiments of Hartmann[17] demonstrate "electron hole" conduction, and he estimated the concentration of holes in his samples to be 10^{-5} mole per mole of UO_2.

The increase in the valence of uranium at some site in the sublattice from 4 to 5 (or 6) will add one or two electron holes per atom. At equilibrium, there can be some transfer of electrons from the valence bonds to quasi-free levels with the formation of holes. This can be symbolically written as

$$\epsilon(\text{valence in } UO_2) = \ominus + \oplus \qquad (1)$$

where, following the notation of Hauffe,[18] $\ominus$ stands for quasi-free electrons and $\oplus$ denotes electron holes. The experiments by Hartmann[17] suggest that the quasi-free electrons occupy high energy states in the solid and are not available for conduction at low voltages or field strengths. One may apply the Law of Mass Action, as Wagner[2] has done, and write the equilibrium-constant expression

$$K_1 = [\ominus]\,[\oplus] \qquad (2)$$

where the brackets denote concentration of each defect.

Hauffe[19] found the electrical conductivity of UO_2 at 1000°C to be relatively insensitive to oxygen pressure. Meyer[20] observed a fourfold increase in conductivity after vacuum-fired UO_2 compacts were annealed in O_2 at 500°C and 100 mm pressure. Using Hauffe's notation for such reactions, the addition of excess oxygen may be represented by the equation

$$UO_2 + \tfrac{1}{2}O_2(g) \rightleftharpoons (O_{\bullet}^{=}) + 2\oplus \qquad (3)$$

where the symbol $O_{\bullet}^{=}$ stands for a doubly charged interstitial ion.

Using the Law of Mass Action to treat the small concentration of these

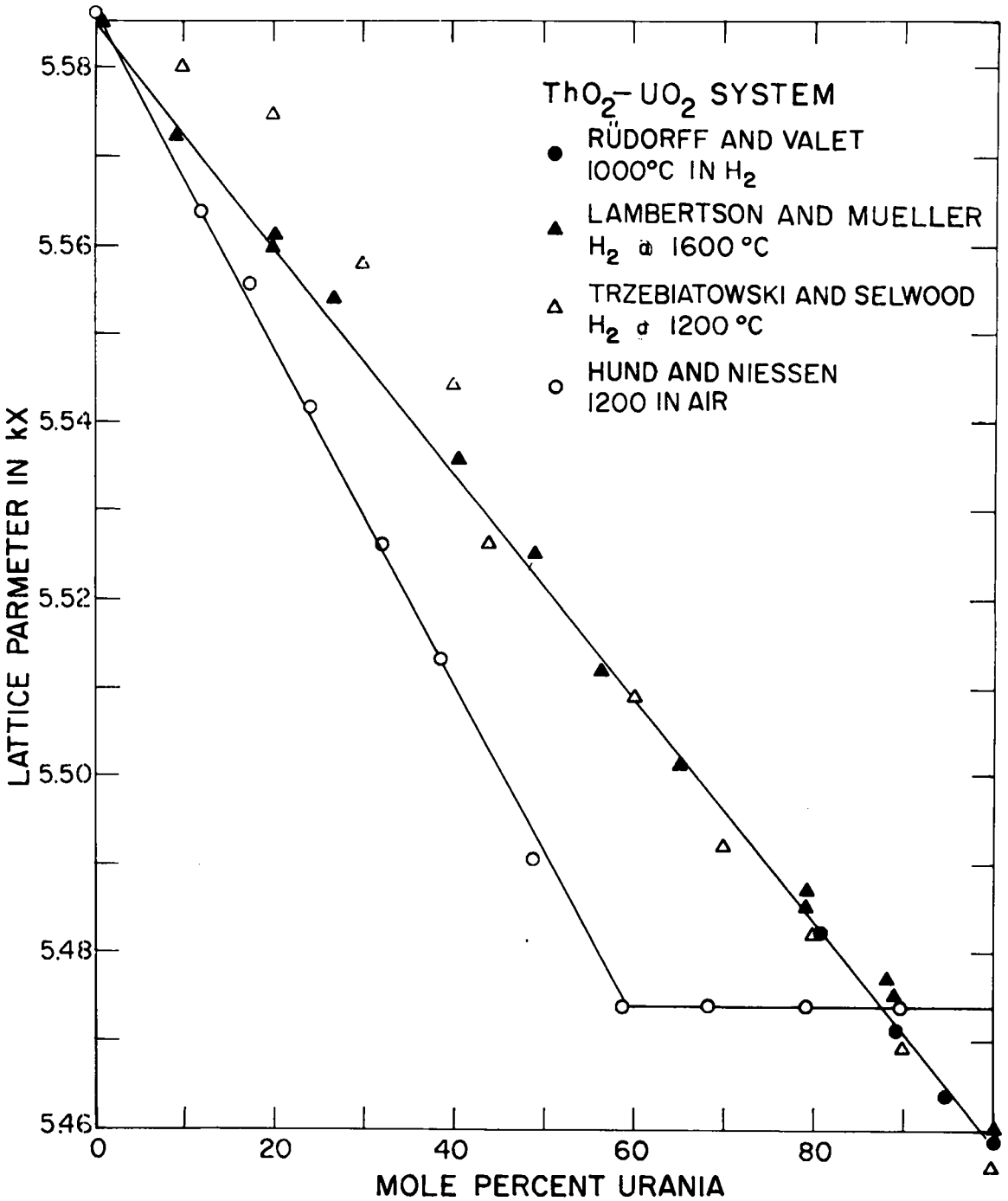

Fig. 1 Variation of Lattice Parameter with the Mole Fraction of UO_2 in Urania-Thoria Mixtures. Hund and Niessen[14] partially oxidized their solid solutions by annealing in air.

defects, the equilibrium constant for this reaction may be written as

$$K_2 \equiv \frac{[O_{\bullet}] \; [\oplus]^2}{(pO_2)^{1/2}} \tag{4}$$

where the brackets denote the concentration of that specie of defect. Since two electron holes are formed for each interstitial oxygen, this equation can be arranged to give

$$[\oplus] = \sqrt[3]{2K_2} \; (pO_2)^{1/6} \tag{5}$$

Thus, if the conductivity is roughly proportional to $[\oplus]$, a millionfold change in oxygen pressure will only change the conductivity tenfold. The experimental observations cited above appear to be in agreement with these arguments. At low oxygen pressures (i.e., in vacuum) the changes in conductivity may be very small if the equilibrium concentration of positive holes given by Eq. 2 is large in comparison with the excess or deficit in oxygen ions. This is undoubtedly the explanation of Hauffe's result.[19]

2.3 Oxygen Pressure Dependence

There are several equilibrium reactions which dictate the pressure dependence of the reaction rate. The basic assumptions in these considerations are: (1) that equilibrium concentrations of lattice defects exist at the metal-oxide and the gas-oxide interfaces; (2) that equilibrium is rapidly attained at the outer interface between the bulk oxide and the gas phase as well as between the metal and bulk solid at the other interface; and (3) that rate (which is diffusion-controlled) is determined by the gradient of lattice defects across the film.

If the external oxygen pressure exceeds the equilibrium decomposition pressure, one can, by neglecting the details of absorption, etc., write the same over-all reaction for the oxide-gas interface as that expressed in Eq. 3. Then Eq. 4 can be written as

$$[O_{\bullet}^{=}] = \sqrt[3]{K_2/4} \; (pO)^{1/6} \tag{6}$$

The concentration of interstitial oxygen ions will be much smaller at the metal-oxide interface since they are consumed there to form the dioxide. This concentration is unaffected by external gas pressure. Thus a gradient exists across the film which increases with the sixth root of the oxygen pressure.

The experimental data of Perkins[21] and Wright and Waber[22] indicate that the rate increases with the gas pressure. The data by Perkins indicate a fifth root dependence, whereas those of Wright and Waber increase with the fourth root of the pressure. These experiments were carried out at relatively high temperature, namely, 260 and 220°C, respectively. The higher oxides of uranium are usually present in the film at these temperatures, and this may account for the larger observed dependence on external gas pressure than the predicted value of one-sixth.

3. OXIDATION BY DRY AIR AND OXYGEN

The published data[23,24] suggest that the reaction of uranium with nitrogen proceeds very slowly at temperatures as high as 400°C, so that to the first approximation, nitrogen can be ignored in discussing the behavior of uranium at temperatures below 200°C. For this reason, the reaction with dry air and with oxygen can be discussed under a common topic.

Many experiments have been run at temperatures below 100°C in an effort to get a further insight into the complex behavior of uranium. Such temperatures are also of interest with regard to handling and storage problems. At high temperatures the gross behavior of uranium appears to be considerably more uniform than at moderate ones.

3.1 Experiments below 100°C

In the early stages of the oxidation of uranium and beyond the interference color range of oxide thickness, the oxide is rather protective. The increase in weight generally follows a parabolic growth law. At oxide thicknesses* of about 750 Å, corresponding to an oxygen pickup of 10 $\mu g/cm^2$, oxide fracture becomes important. The fracture does not lead to deep fissures but rather to the formation of flaking parallel to the metal surface. Fracturing could be expected, since on a mole-for-mole basis UO_2 occupies 1.97 times as much volume as the metal. The resultant highly compressive forces in the surface lead to outward buckling of the oxide layer. Near the metal surface adhesion is apparently greater than the cohesion in the oxide, and "voids" form parallel to the metallic surface. These subsequently open, permitting the access of new oxidant, and since the diffusion-path length is considerably reduced, oxidation proceeds more rapidly locally. As the crack

*Corresponding amount of metal consumed is about 390 Å.

grows laterally in the oxide, there is an increase in the area which is available for the more rapid oxidation, and, consequently, an over-all increase of the rate with time can be expected.

Data obtained with uranium exposed at low temperatures to air which is dried (i.e., in contact with) with P_2O_5 indicate that such an increase in rate occurs. Note that the slope on the log-log plot of Fig. 2 changes from just over 0.5 to slightly over 2. The second portion of the curve has been called "time-squared behavior." This behavior was formerly ascribed to depletion of the absorptive capacity of the desiccant, but more recent experiments with several desiccants, some of which were replaced frequently, have led to the discard of this suggestion.

The proposal that the accelerating rate of attack associated with the time-squared behavior is due to a progressive lateral fracture and exposure of a thin adherent layer to further oxidation is given support by the fact that the maximum amount of oxidation cannot exceed that which would have formed if the oxidation were only controlled by this thin layer throughout the entire time of exposure and the remaining oxide which formed had spalled off, or at least had not interfered with the progress of the reaction. Although a diffusion mechanism is assumed to operate in this thin adherent layer, if the layer were constant in thickness, the oxidation would be limited by the rate of entrance of anions into the film and their diffusion inward, i.e., interface-controlled. The rate would then be constant and a linear law would be observed. Note that in Fig. 3 a linear growth line, superimposed on Fig. 2, is an upper bound to the broken curve, and that the rate indicated by the data declines at long times, suggesting that fracture has occurred once over the entire surface. Even if subsequent fractures do occur after the oxide has again grown within an exposed area to the unstable thickness of 750 to 1000 Å, the linear-law extrapolation will not be exceeded since the local rate in this newly thickened area will be less than in the thin adherent film.

Photomicrographs have been taken of a specimen exposed at 57°C to dry air at two stages after the fragmentation had begun. The two photomicrographs in Fig. 4 are of the same area and illustrate the progressive fracture and fragmentation of the oxide layers. Although it may not be obvious from this figure, the oxide curls away from the metal, and rather "dished" rectangular pieces of oxide are detached from the metal.

A statistical study has been made of the first and second branches of weight-gain curves which exhibited this time-squared behavior to determine if there were any effects due to impurities. Duplicate specimens of three different lots of metal were exposed to air dried with P_2O_5 at 75°C. One lot of metal was also tested which had been rolled in three slightly different ways. Duplicate specimens of the as-rolled and the annealed (recrystallized)

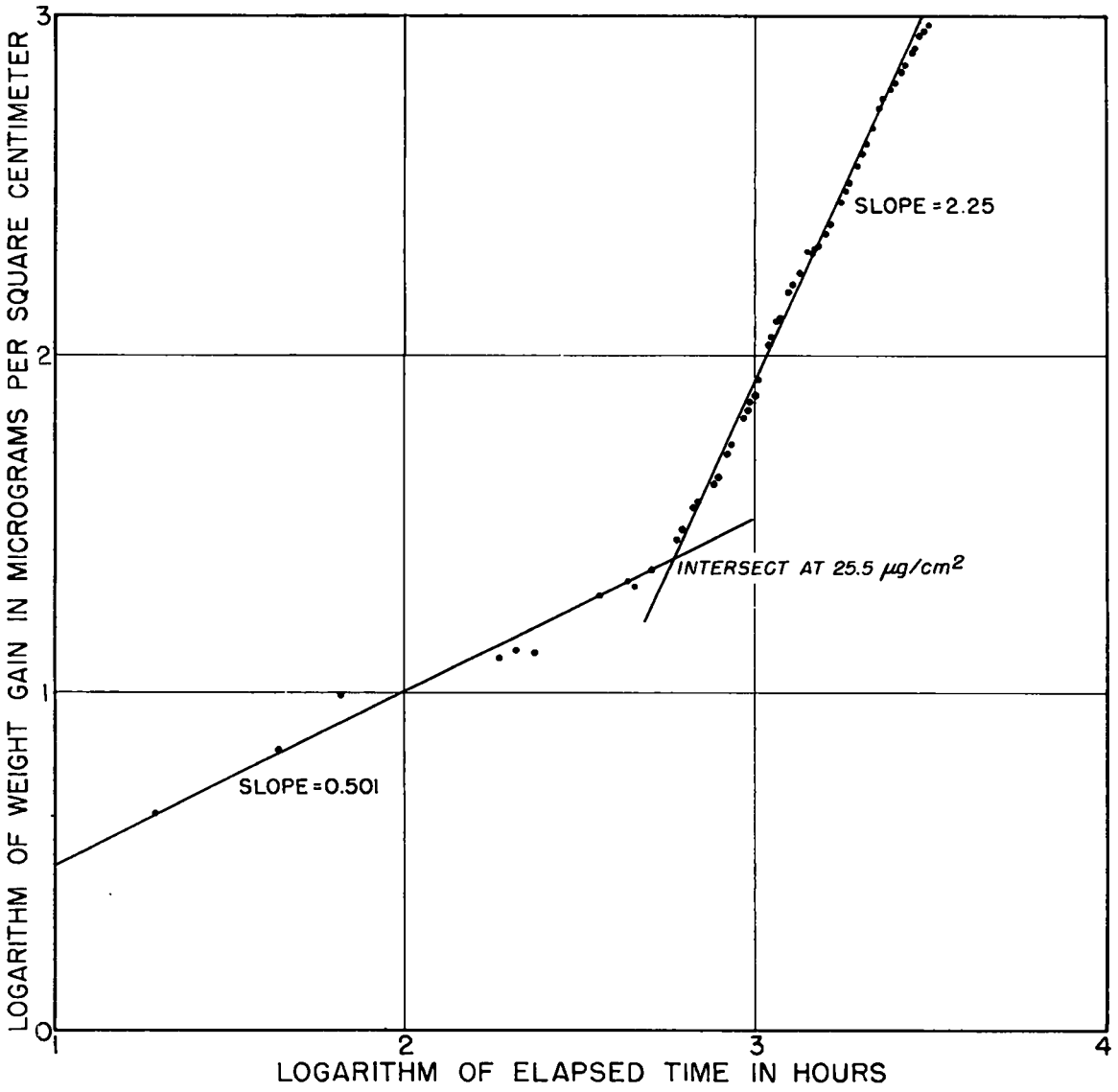

Fig. 2 The Increase in Time Dependence during the Oxidation of Uranium by Dried Air at 57°C. The accelerating attack persists for >2000 hr.

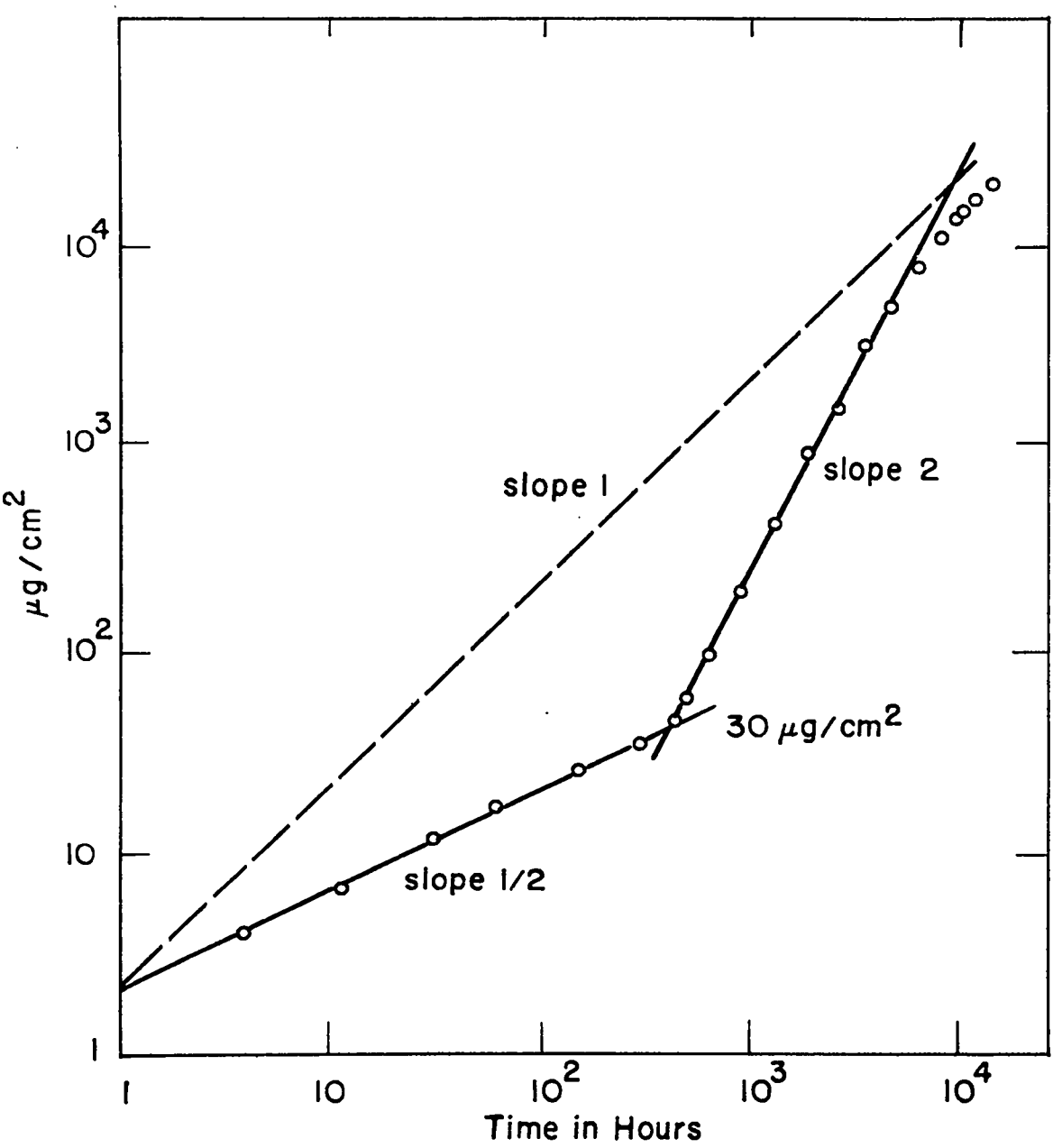

Fig. 3 Graph Similar to Fig. 2 with an Imposed Constant-Rate Curve.

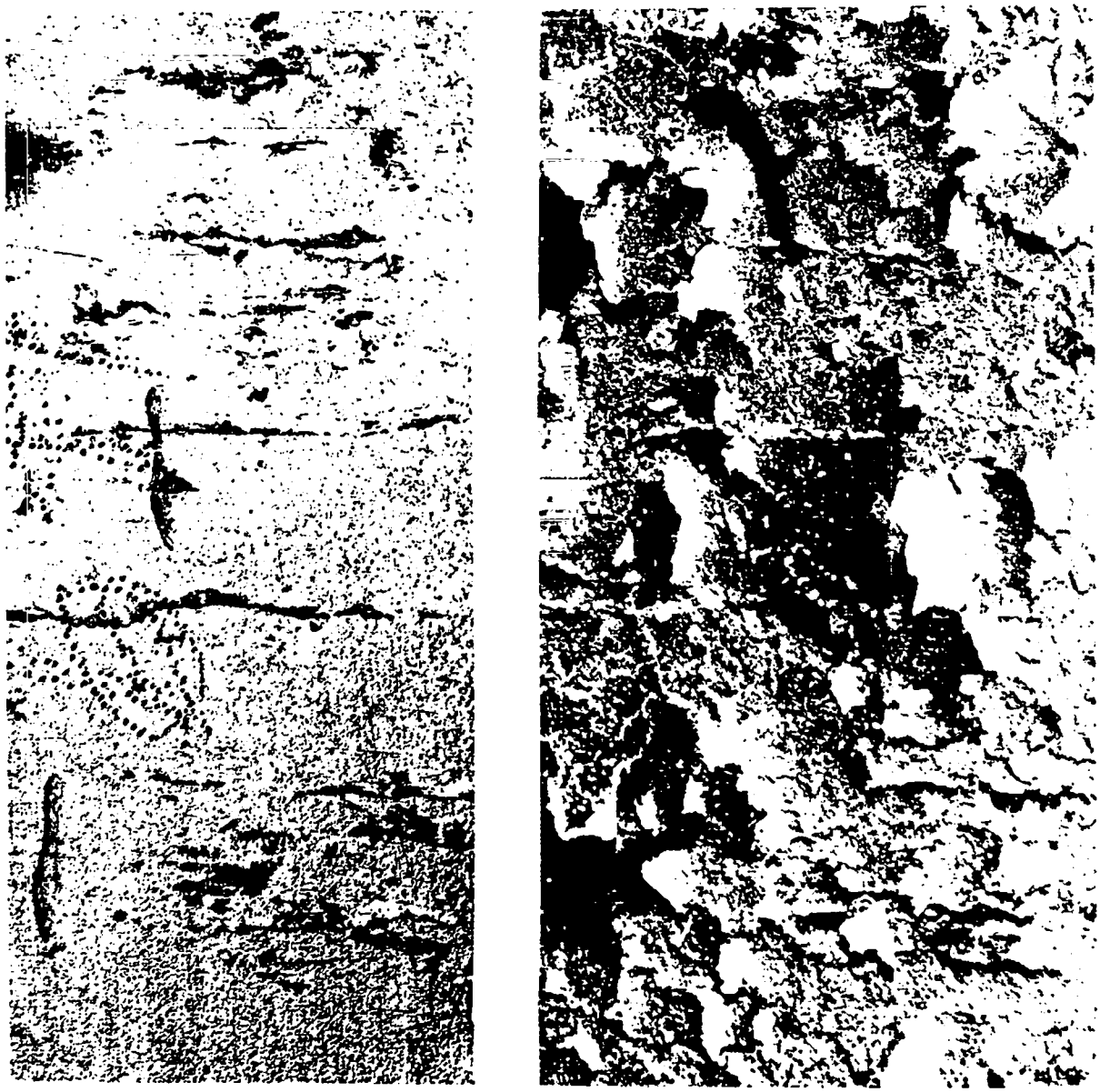

Fig. 4 Photomicrographs of the Oxide Surface during Oxidation by Dry Air. Magnification 50X.

metal were also exposed to dried air at 75°C. Analysis of the data suggests that there were no significant effects clearly due to impurities. Since the behavior of the annealed metal was similar to that of the as-rolled metal, there would appear to be little effect due to the fabrication procedure. Some of these results are presented in the following table. The exponent in the

TABLE 3.1

STATISTICAL SUMMARY OF TIME-DEPENDENCE DATA
RELATING TO THE OXIDATION OF URANIUM IN DRIED AIR AT 75°C

Metal Used	No. of Runs	Av. Initial Slope	Av. 2d Slope
Different lots, various treatments	6	0.465	2.23
Same lot, different treatment	12	0.621	3.66
Pooled data	18	0.569	2.98

time-squared portion was higher than 2.

The variation between the rate constants of duplicate runs in the initial portion of the curves was large and tended to mask any real effect of impurities. However, the rate constants (expressed in terms of micrograms per square centimeters and hours) for the second portion of the curves ranged only slightly and are presented below. These data suggest that the second rate constant, which depends rather strongly on the details of the fracturing process, is virtually independent of the composition or previous history of the metal. It might be expected that the oxide layers could form without too much regard for the nature of the metal, particularly if the impurities in uranium were not soluble in the dioxide. Thus uniform rates which did not reflect the history of the metal could be obtained.

TABLE 3.2

STATISTICAL SUMMARY OF RATE-CONSTANT DATA
RELATING TO THE OXIDATION OF URANIUM IN DRIED AIR AT 75°C

Metal Used	No. of Runs	Av. Rate Constant	Smallest	Largest
Different lots, various treatments	6	7.0×10^{-3}	6.17×10^{-3}	9.02×10^{-3}
Same lot, different treatments	11	4.86×10^{-3}	2.25×10^{-3}	14.7×10^{-3}
Pooled data	17	5.61×10^{-3}	2.25×10^{-3}	14.7×10^{-3}

3.2 Oxidation by Oxygen at 185°C and Higher Temperatures

The studies of Wathen and Perkins are quoted in Los Alamos Scientific Laboratory report LA-1524 (November 1952). Some of our results on time dependence and the effect of thermal cycling are also cited there. For brevity these will not be repeated here.

However, there are further data available from some of our experiments conducted at temperatures at 185°C and above, using a vapor thermostat. In the graph of Fig. 5, the oxygen consumed per square centimeter of specimen surface is plotted versus time. The two-slope character of these log-log plots suggests that a change in mechanism occurs.

It is interesting to note that Wagner has suggested that the decrease in activation energy (cf. the Arrhenius plot of Fig. 8 in LA-1524) at higher temperatures in any reaction can be explained by a sequence of reactions in which, as an essential step, a small amount of intermediate compound is formed. Such a compound might be the tetragonal oxide ($UO_{2.33}$). The proposed steps in that case would be

$$U + O_2 \longrightarrow UO_2 \longrightarrow \text{tetragonal} \longrightarrow UO_{2.66} \qquad (7)$$

The inner part of a high-temperature film would contain dioxide, the exterior part, U_3O_8. Such a change in composition of the oxide as it grew could also explain the dual-slope character of Fig. 5. When one run was interrupted after 1 hr, only UO_2 could be detected by X-ray diffraction. In general, however, the over-all oxygen content was higher in tests of longer duration. In four runs at 220°C the oxygen/uranium ratio, as derived from the consumption of oxygen, was 2.45, 2.45, 2.39, and 2.41, and in each case the presence of dioxide plus the tetragonal oxide was demonstrated. These data imply that the tetragonal phase may have a composition nearer to U_2O_5 than to $UO_{2.33}$.

As a final remark, ignition of 2-mil uranium sheet was observed in pure oxygen at 275 and 344°C.

4. EFFECT OF MOISTURE ON AIR CORROSION

As previously mentioned, small amounts of moisture in the air very significantly increase the corrosion rate. Our experience indicates that increasing the moisture content above approximately 1% relative humidity has little effect in further increasing the corrosion. Even though initially there may be differences, these are largely wiped out at the end of a month or two. To further confirm these observations made at moderate relative humidities, the effectiveness of two commercial desiccants was studied. The equilibrium vapor pressure over a mixture of $CaSO_4$ and its hemihydrate was

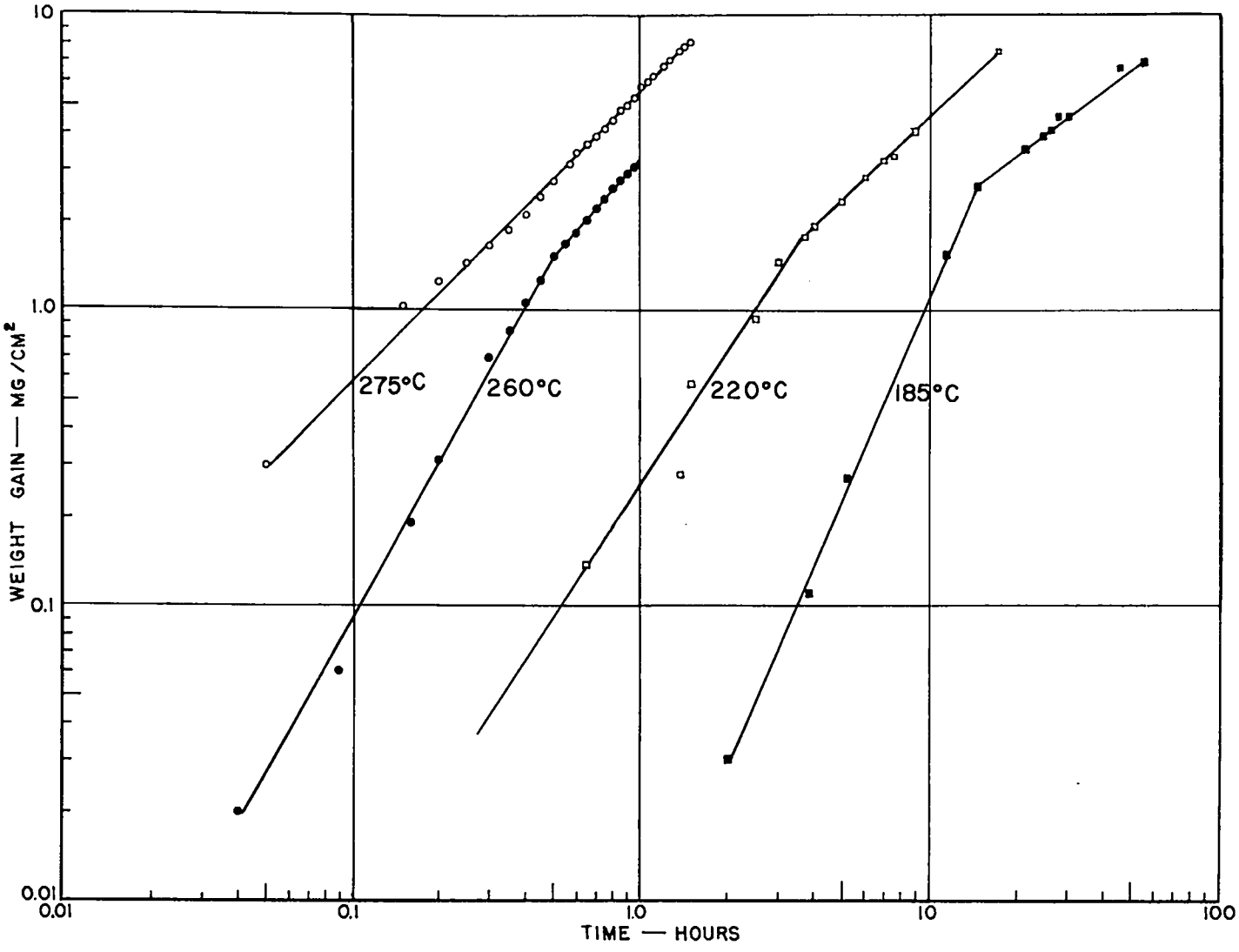

Fig. 5 High-Temperature Oxidation of Uranium in Oxygen. The reduced rate may be due to formation of higher oxides and changed mechanism.

0.023 atmos. at 100°C or approximately 2% relative humidity. Two compounds which would dry a gas by reacting with the water were also tested. A typical set of weight gains obtained with exposing high-purity uranium to air at 75°C in contact with the desiccant are shown in Table 4.1.

TABLE 4.1

EFFECTIVENESS OF SEVERAL DESICCANTS

	Wt. Gain (mg/cm^2)		
Desiccant Employed	100 hr	700 hr	5000 hr
$MgClO_4$ (anhydrone)	0.016	0.039	0.56
CaH_2	0.008	0.055	0.54
Na_2O_2	0.014	0.070	0.54
$CaSO_4$ (drierite)	0.065	1.95	10.8
Control			
50% r.h.	0.51	2.65	11.1

The three compounds $MgClO_4$, CaH_2, and Na_2O_2 gave surprisingly similar results, whereas the $CaSO_4$ was not very much more effective than adding no desiccant and permitting the air to retain a high moisture content.

4.1 Effect of Impurities

Characteristically, the corrosion of uranium does not yield very reproducible weight gains. For this reason, statistical analysis of the data is frequently necessary. The effects of rolling procedure and impurity content have been examined, using a test plan rather similar to that discussed in connection with corrosion by dry air. Although some differences were brought to light by this analysis, the details of rolling and annealing seemed to have much less effect than the lot or sheet of metal from which the metal was taken. This suggests that the chemical analysis of the metal plays an important role.

To study this more thoroughly, unalloyed uranium metal from four different sources was tested at 75°C in air which contained 50% relative humidity. Then large amounts of the common impurities which occur in uranium were added to a single high-purity stock. The results of these tests with moist air when plotted on log-log paper are given in the following table.

TABLE 4.2

COMPARISON OF THE EFFECT OF PROCESSING IMPURITIES AND ALLOY ADDITIONS ON THE CORROSION OF URANIUM

Metal Used	Slope	Logarithmic Intercept	Wt. Gain (mg/cm^2) 100 hr	Wt. Gain (mg/cm^2) 1000 hr
Electrolytic (B-211)	1.47	−4.00	0.51	2.4
Selected Derby casting (3A-157)	1.03	−2.90	0.096	3.60
Center cut Dingot (A-1)	0.88	−2.14	0.135	2.25
Old Hanford extruded (D-199)	1.10	−2.19	0.096	2.00
Control Stock	1.07	−2.92	0.12	1.9
5600 ppm carbon	0.94	−2.60	0.18	1.8
440 ppm iron	1.0	−2.70	0.17	1.75
536 ppm nickel	1.14	−3.04	0.175	2.4
520 ppm silicon	1.27	−3.21	0.22	2.6
500 ppm copper	0.94	−2.76	0.11	1.8
Repeat of D-199 as control	1.14	−3.20	0.115	2.15

The differences were much smaller than was anticipated, and the data in this table suggest that the impurity content has very little influence on the gross corrosion behavior. It is possible, however, that the corrosion rate might be smaller (or larger) if the impurity content were significantly less than in these samples. These data also suggest that small variations in the corrosion test procedure may be of major importance.

For comparison purposes, the data for uranium (from four sources) exposed to dry air at 75°C in contact with $MgClO_4$ are presented. These data

TABLE 4.3

COMPARISON OF THE CORROSION OF VARIOUS URANIUM FEED MATERIALS

Metal Used	Wt. Gain (mg/cm^2) 100 hr	Wt. Gain (mg/cm^2) 1000 hr
Electrolytic (B-211)	0.007	0.053
Selected Derby casting (3A-157)	0.0115	0.053
Center cut Dingot (A-1)	0.0145	0.075
Old Hanford extruded (D-199)	0.0135	0.053

also demonstrate the large difference in corrosiveness of dry and moist air.

5. REACTION WITH WATER

The reaction with water is complicated, and it has been difficult to interpret some of the results since certain hydroxides (or hydrates) are suspect; unfortunately, their X-ray patterns and chemical properties have not been well characterized. The behavior of uranium with respect to water in its various forms--aqueous solutions, water vapor in a moist inert gas, or steam--is rather similar and is discussed in the following subsections.

Although one might have discussed corrosion by moist air here, the behavior in this medium is sufficiently different from that in either dried air or water to merit special attention. For example, it is known that oxygen hinders the attack of uranium by water.* Only UO_2 has been detected after exposure to moist or dry air below 100°C, whereas UH_3, as well as compounds with appreciable amounts of U^{+6}, have been observed to form at low temperatures in cases where water vapor is the principal oxidant.

5.1 Reaction with Hot Water

Much of J. E. Draley's data and his observations of the effect of oxygen on the corrosion rate of uranium is contained in Los Alamos Scientific Laboratory reports LA-1381 (December 1948) and LA-1524 (November 1952). For this reason, they will not be discussed here.

A number of runs have been made at this Laboratory using purified water at 50°C in a gas-tight system.[25] Material balances have been made. Several important observations made during these tests are: (1) the yield of hydrogen was less than theoretical for the formation of UO_2; (2) the corrosion products contained several percent less uranium by weight than did UO_2; (3) the corrosion products were hygroscopic and oxidized readily at room temperature; and (4) a few tenths of a percent of methane was detected in the gas phase. The CH_4, since it increased with time, apparently arose from the reaction of water with the small amount of uranium monocarbide normally present in uranium. A delay or an incubation period was noted in seven of the eleven runs. The rates were not very reproducible despite the precautions taken. Some of these data are given in Table 5.1.

---

*Since the corrosion of uranium is under anodic control and excess oxygen will tend to reduce the anode area associated with oxygen-depleted regions, the reduction of the rate of attack with increasing oxygen is understandable.

TABLE 5.1

VARIATION OF RATES AND DELAY PERIODS IN A SERIES OF EXPERIMENTS WITH CAREFULLY PURIFIED WATER

Run No.	Initial Rate (cc $H_2/cm^2/hr$)	Delay (hr)	H_2 Yield (%)	Wt. of Oxide less Calc. Wt. (%)
M-10	0.0481	250	--	0.4, 0.5
M-11	0.07	None	64.5	3.6, 4.9
M-12	0.067	225	82.7	--
M-13	0.0017	None	23.4	1.7
M-14	0.0019	160	102.8	1.7, 6.0
M-16	0.0120	None	--	--
M-17	0.0078	15	64.6	2.6, 4.3
M-18	0.02	60	87.1	1.5
M-19	0.025	50	82.2	2.2
M-20	0.033	850	48.0	5.6
M-23	0.044	None	91.6	1.7, 6.1

They reflect the sensitivity of reaction to some uncontrolled features of the experiment. The rate was observed to increase with time in runs M-10, M-12, M-18, and M-23. Hoxeng and Rebol[26] observed that the average hydrogen yield in twenty-nine runs at 70°C was 93%.

The uranium was cleaned with 35% HNO_3 before and after reaction with water and weighed on a microbalance. The moles of hydrogen involved in the reaction

$$U + 2H_2O \longrightarrow UO_2 + 2H_2 \qquad (8)$$

were computed for the number of gram-atoms of uranium which correspond to the weight change. This was called the theoretical yield of hydrogen. Much of the uranium dioxide fell to the bottom of the flask during reaction and could be collected by filtration. The weight of uranium on these filter residues was determined by the CMB-1 analytical group and the equivalent weight of pure UO_2 computed. The "oxide" residue was heavier than the theoretical amount of UO_2. The error in these two oxide weights is indicated in the last column of Table 5.1. It was such a residue that was found to be hygroscopic, and this is discussed under the timed series of weighings.

The uranium and water contents of several hypothetical compositions of

corrosion products are listed in Table 5.2, together with the percentages of the theoretical hydrogen yield. One of the possible explanations for the

TABLE 5.2

URANIUM AND WATER OF HYPOTHETICAL CORROSION PRODUCTS

Composition of Product	Uranium Content	Water Content	Hydrogen Yield
UO_2	88.1	--	100
$UO_2 \cdot H_2O$	82.9	5.91	100
$UO_2 \cdot 2H_2O$	77.8	11.75	100
U_2O_3	90.1	--	75
$U_2O_3 \cdot 3H_2O$	81.8	9.3	75
$2U_2O_3 \cdot UO_2 \cdot 4H_2O$	85.6	5.18	80
$U_2O_3 \cdot 3UO_2 \cdot 4H_2O$	84.6	5.12	90

low uranium content and low hydrogen yield is that uranium hydroxides are formed with an average valence less than 4. The uranium valences for the last two entries in this table are 3.2 and 3.6.

The hygroscopic character of the corrosion products was observed in a series of timed weighings which were made after it was found that one could not dry the products to constant weight. A typical graph of the weight increases which occurred within minutes after removal from the desiccator is shown in Fig. 6. At first it was thought that the successively higher weights upon removal were due to the incomplete removal of the adsorbed water. The occurrence of an initial weight after long storage which was larger than the largest moist weight during the previous timed series of weighings suggested that the corrosion products gained weight while in the desiccator. The (extrapolated) initial weight on removal is plotted in Fig. 7 against hours of storage within the desiccator. The slopes of the two types of weight increases are given in Table 5.3.

Chemical analysis of the products from M-20 after the timed weighings gave 83.5% U. The uranium content for M-23 was initially 86.7 and fell to 83.0% after the timed weighings were completed. (Pure UO_2 contains 88.15% U.) Although the products may have slowly adsorbed water from the desiccant, it seems more reasonable that they were being oxidized while in the desiccator.

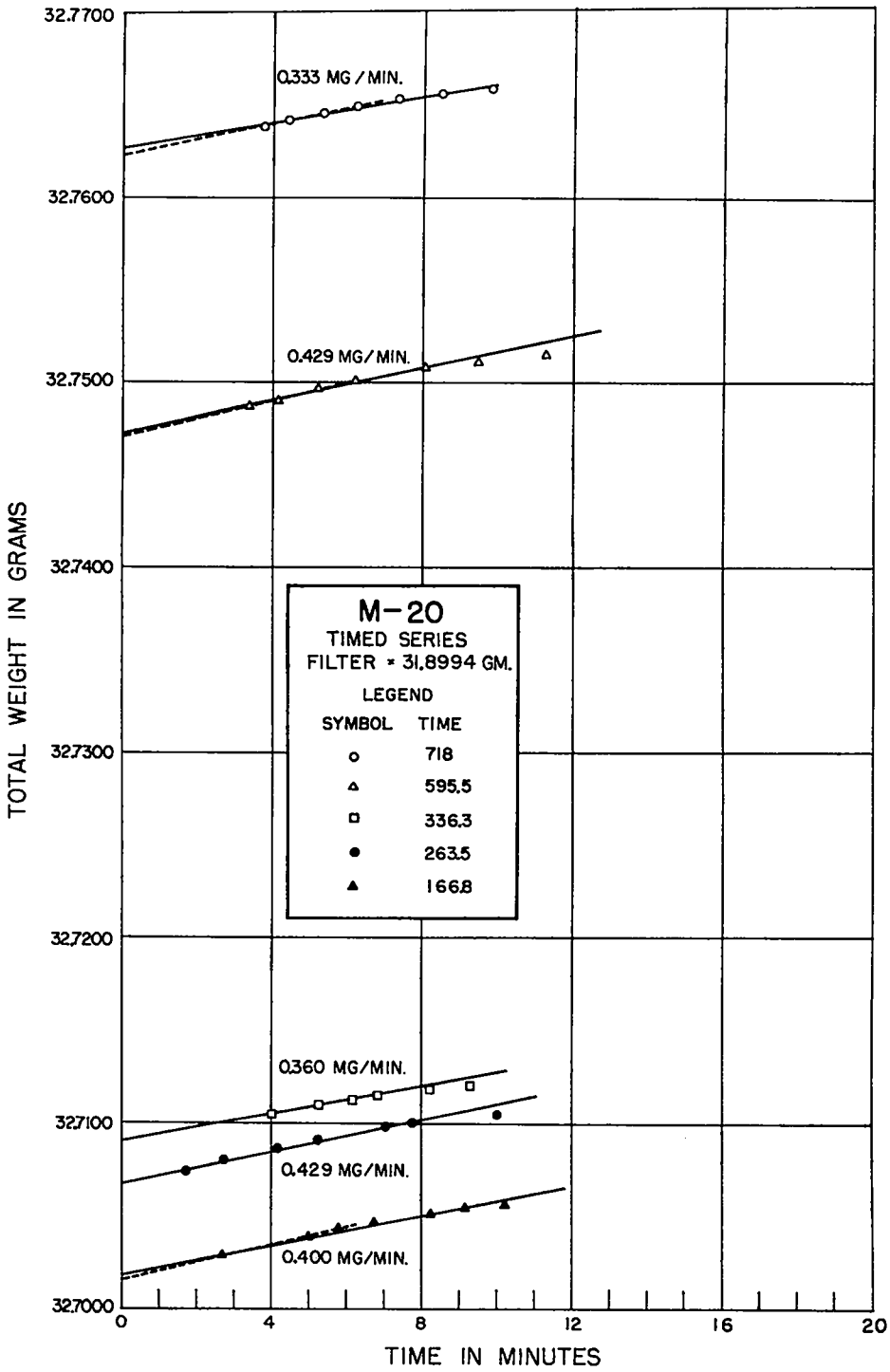

Fig. 6 The Weights of the Filter Residue from Run M-20 as a Function of the Time after Removal from the Desiccator.

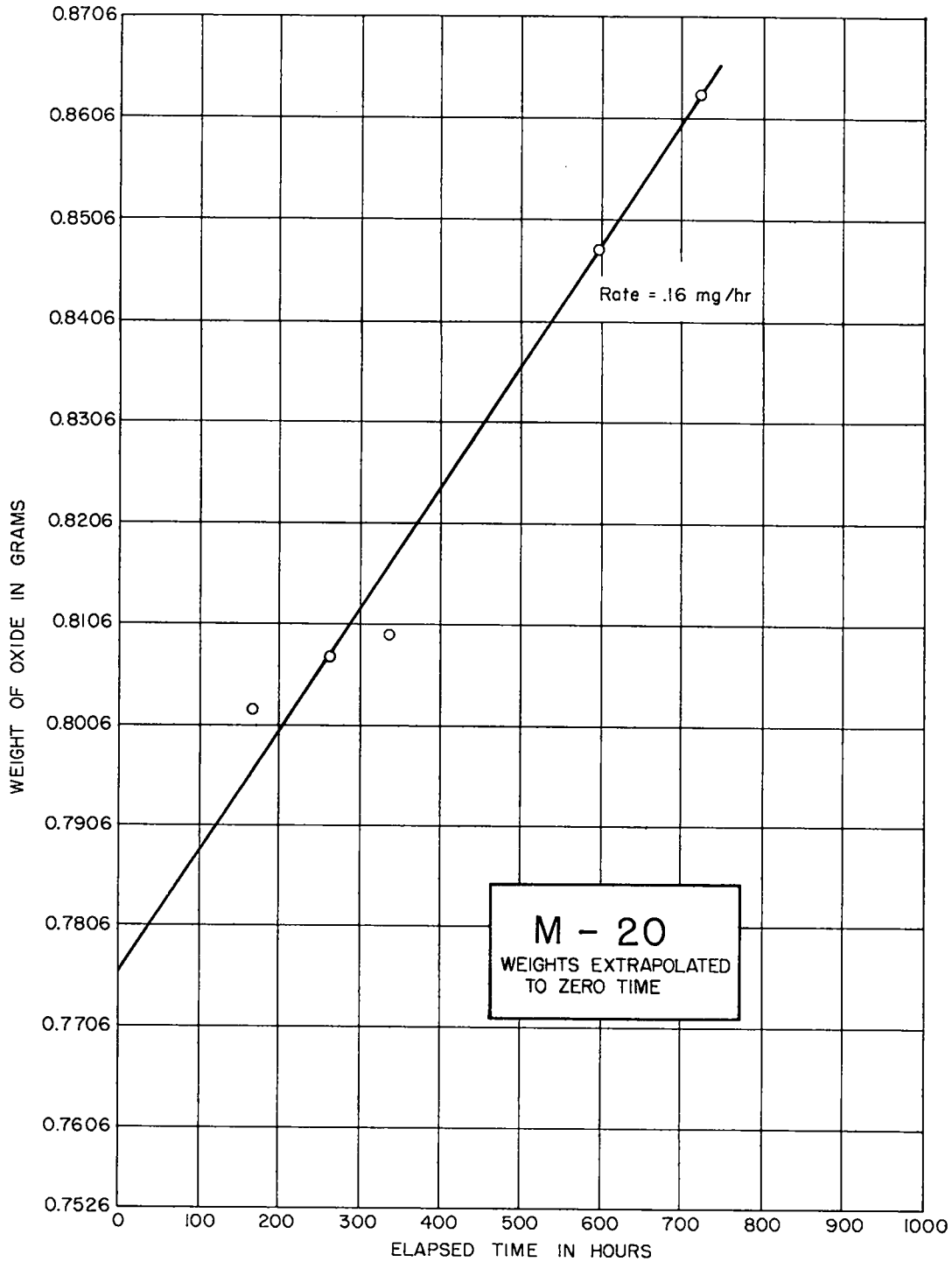

Fig. 7 The Weights of the Corrosion Products as a Function of the Time in the Desiccator.

TABLE 5.3

OXIDATION AND HYDRATION OF CORROSION PRODUCTS AFTER REMOVAL FROM TEST

Run	Rate of Adsorption of H_2O (mg/min)	Rate of Wt. Increase in Desiccator (mg/g/hr)
M-19	0.34	0.018
M-20	0.37	0.206
M-23	0.53, 0.34*	0.145, 0.013*

*Indicates the rates of weight change after a portion of the corrosion product had been removed for analysis.

In recent experiments with uranium in boiling water, the adherent corrosion products were examined by X-ray diffraction within minutes after removal from solution. A number of unidentified lines were observed in addition to those of UO_2. They were similar to the lines of the several $UO_3 \cdot xH_2O$ compounds, but a satisfactory identification has not yet been made.

All of these observations and anomolies can be explained if there was a competition between dioxide-, hydrated dioxide-, and hydride-forming reactions on the uranium surface and if the amount of one reaction in comparison to another depended on a variety of unknown but subtle factors.

5.2 Corrosion in Moist Helium

The reaction of uranium with the water vapor in moist inert gas has been studied over the temperature range of 35 to 100°C and at different relative humidities to determine the effectiveness of adsorbed moisture films. The assumption that the rate will increase proportionally with the surface coverage and with the number of physically adsorbed layers is a reasonable one. Relative humidity may be used as the relative condensation pressure of the adsorbate. Kolodoney and Covert's data[27] have been replotted in accordance with the Brunauer-Emmett-Teller theory of adsorption in Fig. 8. The straight line lends credibility to these assumptions. In this figure, R is the relative condensation pressure, which is the relative humidity in the case of water. It can be shown that if the corrosion rate W is proportional to the surface coverage and W_0 is the rate for a complete monolayer, then the relation between W and R may be written as

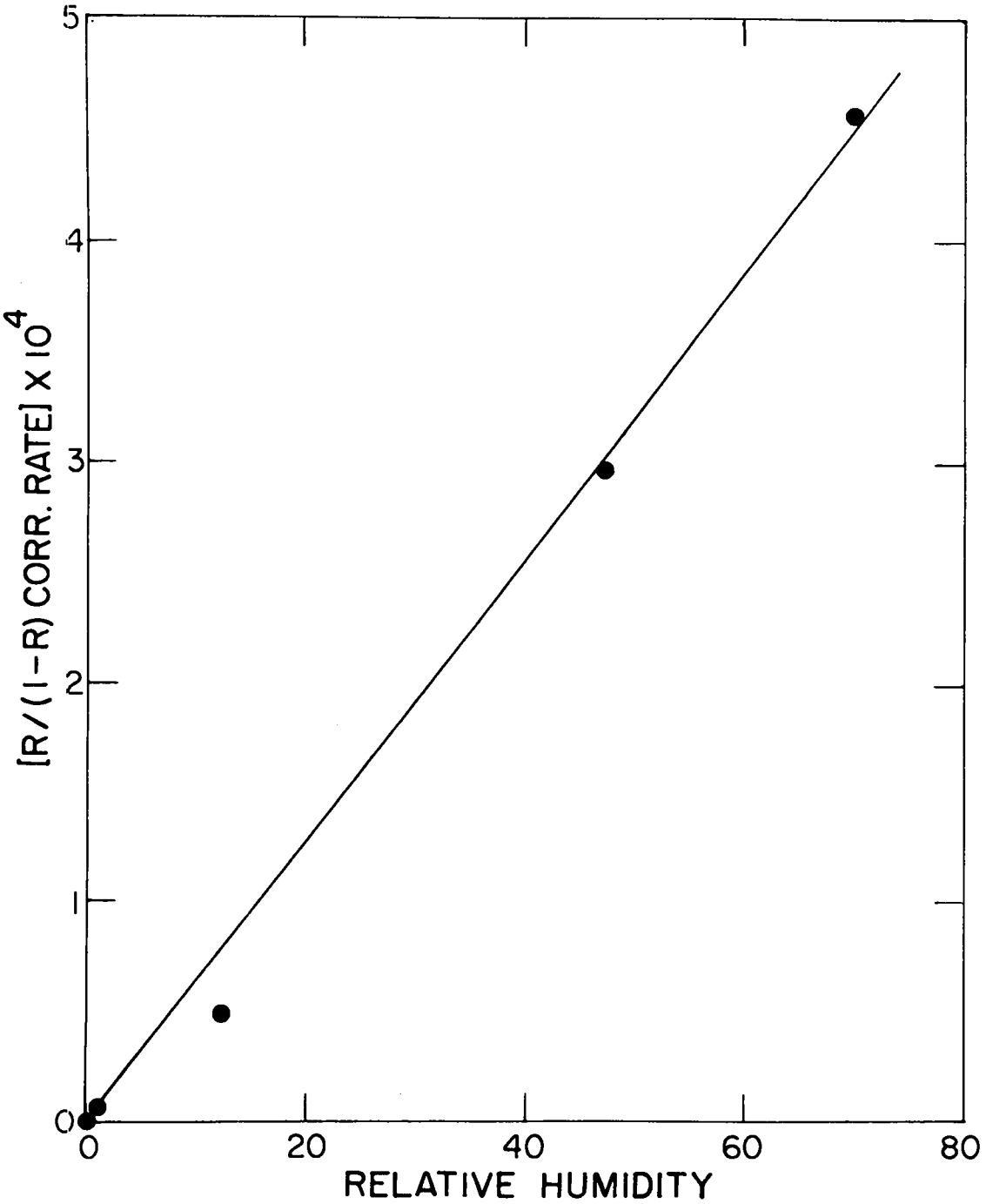

Fig. 8 Effect of Humidity on Corrosion of Uranium at 100°C (assumed to be related to the surface coverage as computed by the Brunauer-Emmett-Teller theory of adsorption).

$$\frac{R}{(1-R)W} = \left(\frac{C-1}{CW_0}\right)R + \left(\frac{1}{CW_0}\right) \qquad (9)$$

Thus one should obtain a straight line by plotting $R/(1-R)W$ against R, the slope being $(C-1)/CW_0$. The heat of adsorption can be derived from the constant C and is estimated from these data to be 22.5 kcal/mole for the adsorption of water vapor on UO_2.

One of the interesting phenomena which have been observed in tests with moist helium is the formation of easily detachable, coherent layers of oxide. In one experiment, eight distinct layers were lifted at the end of the test from the specimen with a pair of tweezers. These layers permitted us essentially to section the oxide film and determine if the film were homogeneous in composition. Chemical analysis of the innermost and outermost layer as presented in Table 5.4 showed that the uranium content of the film decreased as one proceeded outward from the metal interface. The products thus contained less than the stoichiometric percentage of uranium in pure UO_2, namely, 88.15%. The content of water was surprisingly high. If one assumes that the composition can be expressed as $(UO_2 \cdot xH_2O)$, there was more than 100% of material present, namely, 103.1 and 104.9%, respectively. If UH_3 is present, the discrepancy is even larger, since it contains 98.76% U. These low uranium contents can be explained by the presence of higher oxides.

TABLE 5.4

URANIUM AND WATER CONTENT OF CORROSION PRODUCTS FOLLOWING EXPOSURE TO MOIST HELIUM

Layer	U Content (%)	H_2O (%)
Innermost	86.22	5.3
Outermost	84.84	8.7

It was also observed that the outermost layer fluoresced a dark muddy yellow, whereas no fluorescence of the innermost layer was detected. Only uranium compounds containing U^{+6} ions are known to fluoresce.[28] Fluorescence of UO_2 or U_3O_8 has not been observed. This observation of fluorescence suggests that one of the $UO_3 \cdot xH_2O$ phases was present. An X-ray diffraction study of these layers showed only UO_2 in the inner layer. However, a few unidentified lines in addition to those of the dioxide were observed in the outermost layer.

When uranium, after reaction with moist helium, had been stored more than a year in a desiccator containing H_2SO_4, light-yellow products were to be seen on the exterior surface. Petrographic study of this material revealed the presence of $UO_3 \cdot H_2O$ and uranyl carbonate. It is interesting to note that well-weathered uranium or uranium which has been exposed to ground waters also contains uranyl carbonate in the film.

R. J. Bard, of this Laboratory, has measured the area of one of these detached layers by the BET method using methane as an adsorbate. The surface area was 14.1 meters^2 per gram. This surface area can be accounted for by an equal weight of 550 Å cubes. These data suggest that these detached layers are very porous.

In an effort to establish the presence of uranium hydride in the corrosion products, Bard enclosed one of the films in a small evacuated space and measured the pressure at 255°C. It proved to be 6.2 mm Hg. The equilibrium decomposition pressure of UH_3 at this temperature is 25.1 mm. It is more significant that the analysis of this gas by mass spectrometer showed 68% H_2O, 25% CO_2, and the remainder, air and various "background contaminants." No hydrogen could be detected. This was regarded for several years as proof that uranium hydride does not form a significant fraction of the corrosion products. The water undoubtedly came from a hydrated oxide.

Christ[29] reported that $UO_2 \cdot xH_2O$ loses all of its water when heated for 1/2 hour at 200°C and suffers partial oxidation to U_3O_8. According to Aloy,[30] $UO_2 \cdot 2H_2O$ oxidizes slowly in the cold and more rapidly on heating to $UO_3 \cdot H_2O$.

In this connection, we have studied the oxidation of these layers, which proceeded smoothly at 185°C to form U_3O_8. At 200°C, one layer was 85% converted to U_3O_8 in a few hours. At 234°C, oxygen converted one of the layers to 77% U_3O_8 plus higher oxides such as UO_3.

In the course of analysis, samples of these films have been oxidized to U_3O_8 at high temperatures and the water collected. If this water were attributable to the oxidation of the UH_3 which is contained in the film, then approximately 15 to 20 mole % of the hydride would have to be present. Evidence for it has never been found in these films. This large amount of H_2O can be explained more easily on the basis that appreciable amounts of hydrated oxides were present.

Recently it has been demonstrated metallographically that hydrides do form. Figure 9 shows a cross section of the surface of a specimen after 1689 hr exposure to helium containing 50% relative humidity at 75°C. The grey area on the left represents the original surface of the metal. The black material is the plastic mounting. Corrosion has proceeded to the depth of approximately 3 mils in the rounded areas, which are filled with oxide. The triangular-shaped piece has been identified as uranium hydride. The tip

Fig. 9 Photomicrograph of the Surface of Unalloyed Uranium after Exposure to Helium containing 50% Relative Humidity at 75°C for 1689 Hr. The spike has been identified as β-UH_3 by microbeam X-ray techniques. Mechanically polished. Magnification 400X. (Courtesy of C. O. Matthews and C. Olsen, of this Laboratory.)

extends about 10 mils from the rounded area, where it presumably originated. Such nonuniform attack is characteristic of the hydride reaction. This triangular hydride "spike" is imbedded below the surface of the metal and undoubtedly explains why X-ray diffraction of the surface and experiments conducted with detached films have failed to reveal uranium hydride.

One experiment in which uranium was exposed to hydrogen containing 6.5 vol. % H_2O was run at 150°C. Reaction with the hydrogen began within 5 min and localized areas were attacked with the formation of UH_3 beneath a thin oxide film. This experiment is cited to show that some preferential hydriding is possible in moist hydrogen and thus is likely in moist helium. The uneven corrosion attack seen in Fig. 9 is attributable to this cause. Of course, the hydrogen in the case of the experiment with moist helium was derived from the reaction of the uranium with the moisture.

5.3 Effect of Impurities in the Metal

For comparison purposes, data on corrosion of uranium derived from four sources are presented in Table 5.5. Test conditions were 75°C and 50% relative humidity in helium. The effect of these small changes in the impurity

TABLE 5.5

COMPARISON OF THE CORROSION OF VARIOUS URANIUM FEED MATERIALS

Metal Used	Wt. Gain (mg/cm^2)	
	100 hr	1000 hr
Electrolytic (B-211)	1.25	19
Selected Derby casting (3A-157)	1.17	11
Center cut Dingot (A-1)	1.10	18
Old Hanford extruded (D-199)	1.00	33

content seems to be minor.

Three successive runs with two samples from the same rolled sheet (Lot I) of uranium were exposed at 57°C to helium of 10% relative humidity. The duplicate slopes and rate constants for each run are listed side by side in Table 5.6. These results indicate the real reproducibility of the data, since the tests were conducted at different times, and suggest that the results are sensitive to the experimental details of a run.

TABLE 5.6

DUPLICATE VALUES OF RATE DATA FOR REPEATED USE OF SAME SPECIMENS

Slopes		Rate Constants ($\mu g/cm^2/hr$)	
1.02	1.14	0.59	0.34
0.97	0.85	0.75	1.62
0.85	0.76	2.46	6.2

Data are also available from similar experiments at 57°C and 10% relative humidity in which one casting was reduced to sheet by three different rolling schedules. Annealed specimens were also included in the test. All the specimens in this set were tested at the same time. The mean slope

TABLE 5.7

EFFECT OF ROLLING PROCEDURE ON THE CORROSION OF URANIUM IN MOIST HELIUM

Rolling Schedules		Slopes		Rate Constants ($\mu g/cm^2/hr$)		Wt. Gain (mg/cm^2), 1000 hr	
Schedule I	As rolled	1.08	1.05	0.20	0.23	2.7	2.7
	As annealed	0.91	0.51	0.51	4.24	3	3
Schedule II	As rolled	1.07	1.34	0.39	0.07	3	5
	As annealed	1.11	1.18	0.13	0.10	2.5	2.5
Schedule III	As rolled	0.86	1.34	0.42	0.07	2.2	2.2
	As annealed	1.00	1.17	0.21	0.10	2.4	2.4

of 1.05 for these twelve runs is generally somewhat higher than has been observed for the initial reaction in moist helium. These variations in rate constants and slope are not so significant as one might expect in terms of a weight gain at the end of long-term tests but represent the best fit of the data.

Experiments with three different lots of metal also conducted at various times at 57°C and 10% relative humidity gave the following slopes and rate constants.

TABLE 5.8

VARIATION OF RATE DATA WITH DIFFERENT LOTS OF URANIUM

Metal Used	Slopes		Rate Constants ($\mu g/cm^2/hr$)	
Lot II	0.36	0.37	3800	8400
Lot 1023	0.64	0.73	204	71
Lot 2023	0.71	0.65	21	49

These rate-constant data differ somewhat from those obtained in similar runs described above. Although the spread appears large, there is little reason to question the reliability of these data or conclude that there is a real effect due to impurities.

5.4 Reaction with Steam

Dynamic tests have been conducted in this Laboratory using steam heated to 144, 185, and 226°C. The rate of evolution of hydrogen was constant for periods up to 8 hours. X-ray and chemical analysis of the products from the higher temperature run gave UO_2 plus an unidentified constituent, and the chemical analysis showed 59.9% U^{+4} and 24.1% U^{+6}. The hydrogen yield on the basis of these valence changes was 96.5%, which is substantially higher than the value obtained by Wathen.[31] An Arrhenius plot of the data is given in Fig. 10.

6. AQUEOUS CORROSION AND INHIBITION EXPERIMENTS

6.1 Differential Aeration

Although it has been known for a number of years that oxygen reduces the rate of corrosion in water, it has only been within the last 6 months that differential aeration experiments have been conducted. In the first one, polished uranium was immersed in an open beaker and a cover glass brought close to the surface. The metal near the edge of the glass, where there was a supply of oxygen diffusing into the water, was relatively unattacked but the oxygen-starved region near the center became deeply pitted. It was subsequently demonstrated that current flowed between two specimens immersed in water within an H-cell if one specimen was supplied with more oxygen

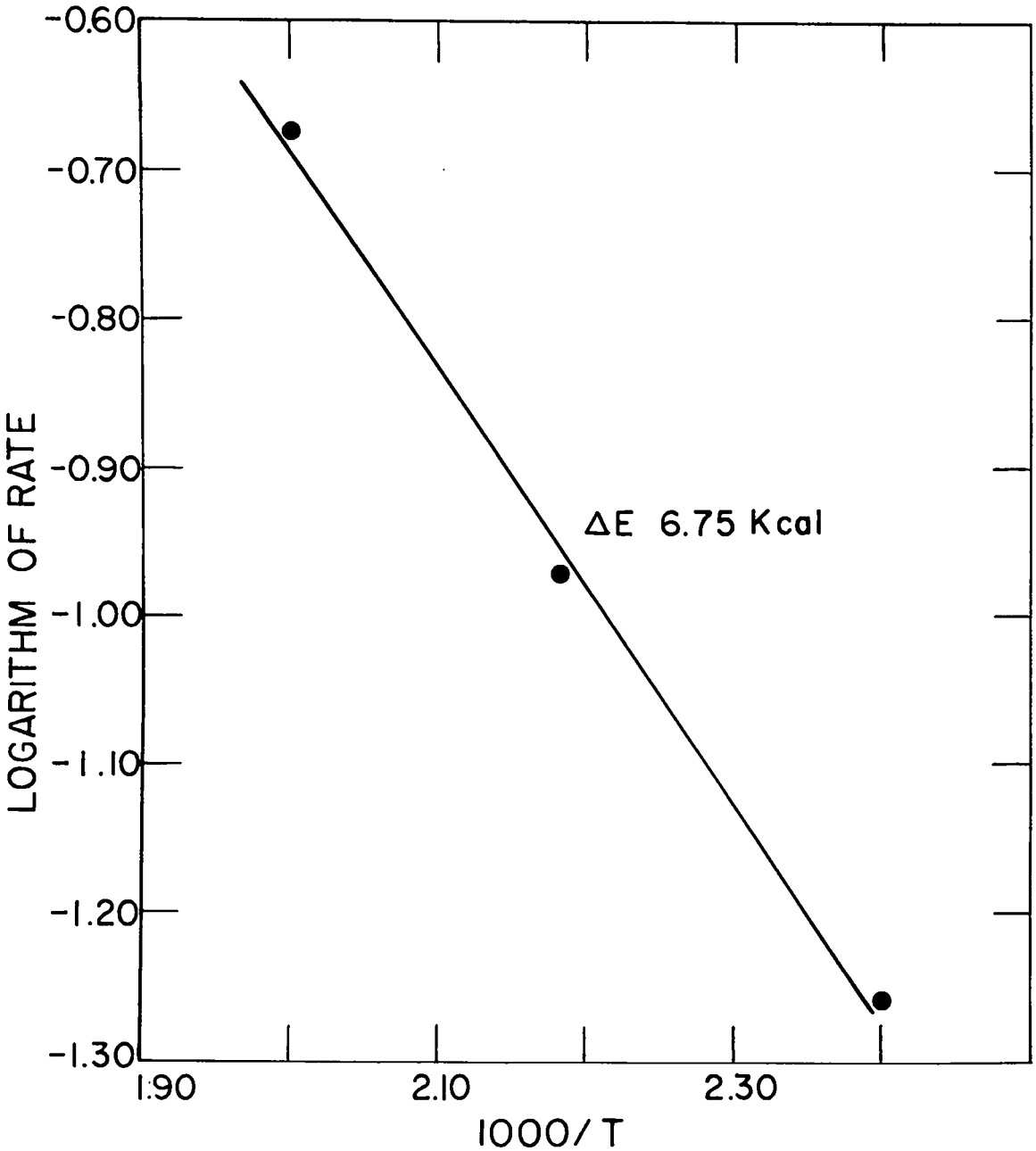

Fig. 10 Arrhenius Plot of the Linear Reaction Rate Constant for Oxidation by Superheated Steam.

than the other. At the beginning of the experiment, current reversal occurred rapidly when the oxygen supply was changed from one side of the H-cell to the other. After about an hour of immersion, the current dropped rapidly to a few microamps on changing the oxygen supply, but the actual reversal was very sluggish. The observed current was of the order of 50 μamps/cm^2 and the anode was the oxygen-depleted side of the cell. Petrochemical analysis of the corrosion products showed evidence of $UO_3 \cdot 2H_2O$ on the specimen exposed for several days to the flowing oxygen, whereas only UO_2 and U were found on the companion piece.

6.2 Inorganic Inhibitors

Various inorganic inhibitors which are known to be effective with iron have been tested with uranium. Aerated solutions containing chromate, molybdate, tungstate, and nitrite were used in the concentration range 10^{-5} to 10^{-3}M. These were only moderately effective; the nitrite ion was the best. Interference colors remained on the surface of uranium after 350 hr at 70°C. However, pitting did occur and thus weight changes do not adequately reflect the protection afforded.

6.3 Dissolution in Nitric Acid

Nitric acid appears to passivate uranium, but slow dissolution does occur. As a basis for comparison, 1 to 2N hydrochloric acid will dissolve uranium pieces 1/8 in. thick within several hours at room temperature, whereas several months would be required with 5N nitric acid at room temperature. Other acids except sulphuric attack uranium rapidly.

Nitric acid has been used by Wathen[31] and by Draley and his associates[32] to remove the film of adherent corrosion products from uranium. Since UO_2 is readily soluble in nitric acid, the sequence of interference colors is passed through when a lightly oxidized specimen is immersed in 5N acid, and the metal remains bright and shiny for considerable periods after the dioxide has been removed. Eventually the surface becomes roughened and deeply pitted.

In experiments made at Los Alamos two constant rates of dissolution were observed in general during a single run; the low initial rate was followed by an increased rate. In Fig. 11, the data of runs T-6, 7, and 8 are plotted as micrograms of metal lost per square centimeter versus the test duration. The initial run can best be represented by two intersecting lines. Re-use of the same specimens in the later runs resulted in higher rates of attack and in a gradual disappearance of the slower initial rate. The

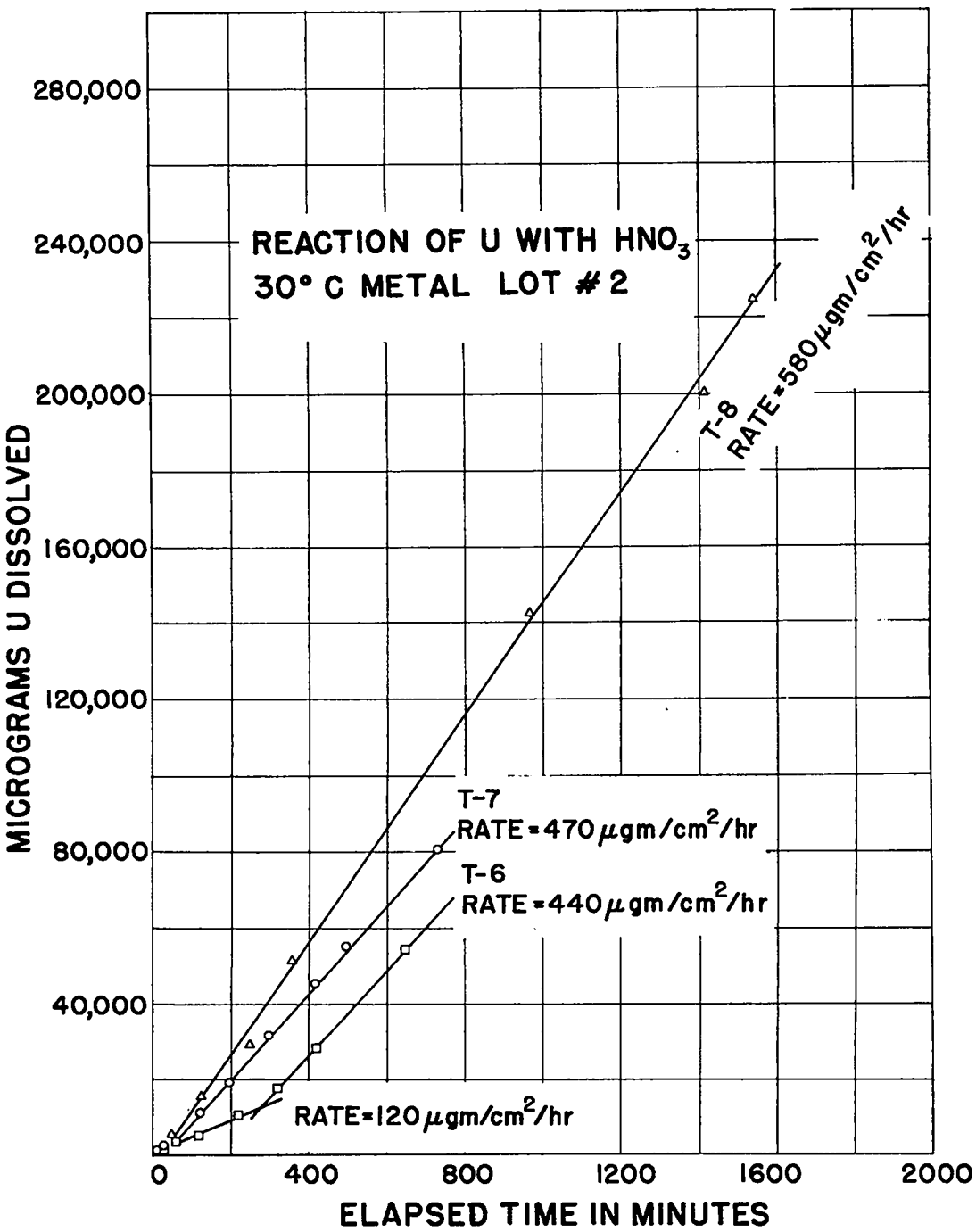

Fig. 11 The Amount of Uranium Dissolved from the Surface as a Function of Test Duration. The same specimens were used for each run. 5.6N nitric acid used.

specimens used for Fig. 11 were repolished and two reaction rates reappeared as shown in Fig. 12. The bilinear character of the reaction curve is related to the impurities, for example, carbon, in the surface of the metal. As the impurity content of the metal stock was reduced, the rates declined and the two slopes merged into one. Typical rate data for the second portion of the curves (not shown in Fig. 12) are:

TABLE 6.1

RATE OF DISSOLUTION* OF URANIUM METAL OF SEVERAL PURITIES FOLLOWING THE INITIAL "PROTECTED" PERIOD

Lot Number	Carbon (ppm)	Iron (ppm)	Rates ($\mu g/cm^2/hr$)
II	600	60	3510
2023	160	630	380 - 2800
D-359	175	125	360

*In 5.6N HNO_3 at 50°C.

The general increase in rate on re-use was undoubtedly due to the surface roughening, since the specimens were not thoroughly repolished between runs. The lower initial rate has been attributed to cathodic protection of the remainder of the metal by the carbide and other inclusions until they were exhausted on the surface. Then the higher rate took over. Deep elongated pits which lie parallel to the rolling direction were observed on removal from solution, as illustrated in Fig. 13. These pits undoubtedly resulted from the dissolution of impurity inclusions which were broken up and aligned in stringers by the rolling procedures, as illustrated in Fig. 14. There were fewer stringers exposed by the partial polishing of the specimens for re-test. Thus the cathodic protection afforded by these was of less duration and the higher rate set in sooner.

7. DISCUSSION

The corrosion behavior of uranium is understood only qualitatively. The detailed quantitative behavior is variable and appears to depend on various conditions prevailing at the surface. However, impurities in the metal or differences in fabrication do not apparently influence the rate. The moisture and oxygen content of the corrosive environment seem to have a much more significant effect.

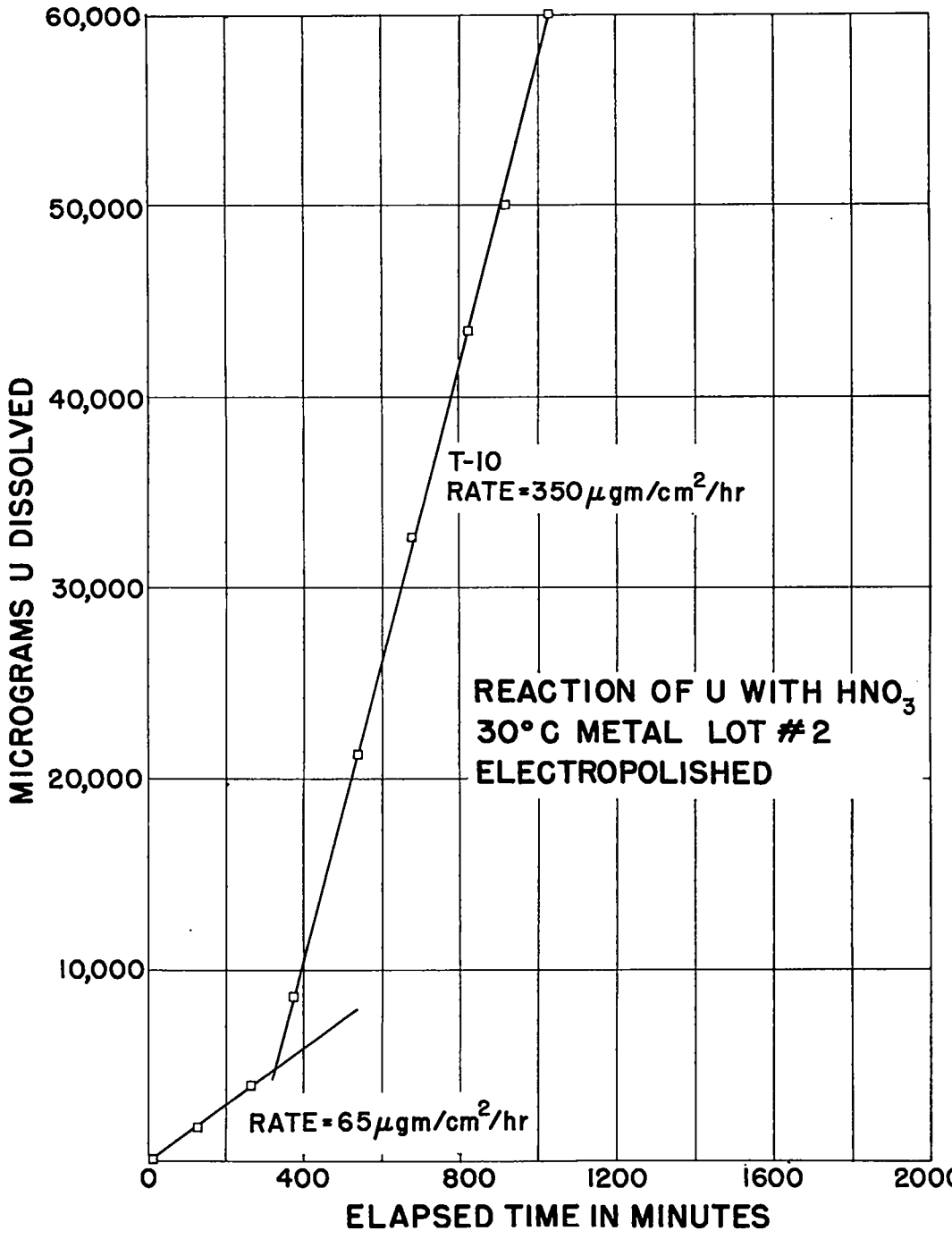

Fig. 12 Reaction of HNO_3 with Same Uranium Specimens from Run T-8 after Careful Re-polishing. Note the reappearance of the initial low reaction rate.

Fig. 13 Photomicrograph of the Corroded Surface of Lot II Uranium after Removal from Test. Run T-23 lasted 1270 min. Conducted at 40°C.
Plate 385-1-1 Magnification about 50X

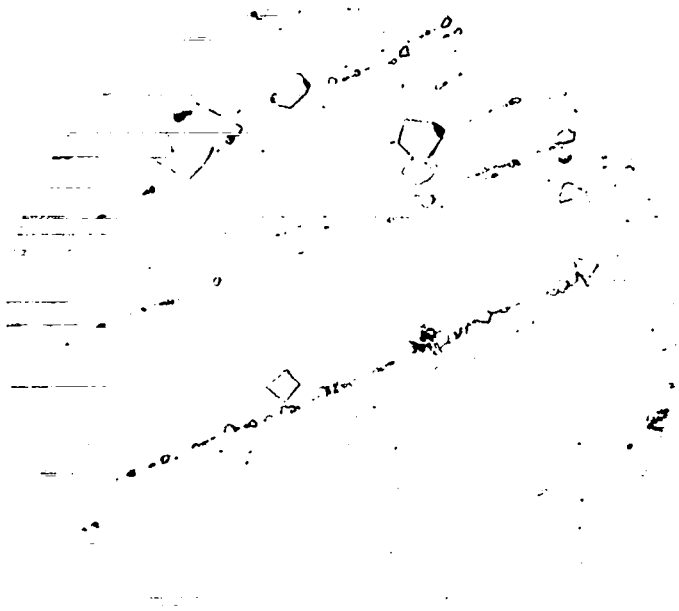

Fig. 14. Photomicrograph of Warm-Rolled Uranium. Illustrates the alignment of inclusions caused by the rolling. Electropolished and unetched.
Plate 353-3-1
Lot II metal Magnification about 500X

The observed variability in reaction rate can be qualitatively explained if a number of competing as well as successive reactions occur simultaneously on the uranium surface, and the rate of several of these is strongly influenced by impurities in the gas. Certainly a number of products such as UH_3, UO_2, and higher hydrated oxides have been observed to form in the presence of air. The several products are in accord with several simultaneous reactions.

REFERENCES

1. C. Wagner and W. Schottky, Z. physik. Chem., B 11, 163 (1936).
2. C. Wagner, "Reactions of Metals and Alloys with Oxygen, Sulphur, and Halogens at High Temperatures," Pittsburgh International Conference on Surface Reactions, pp. 77-82, Corrosion Publishing Co., Pittsburgh, 1948.
3. F. Gronvold, J. Inorg. & Nuclear Chem., 1, 357 (1955).
4. P. Perio, Bull. soc. chim. France, 20, Series 5, 256 (1953).
5. H. Hering and P. Perio, Bull. soc. chim. France, M 351 (1952).
6. F. Hund and U. Peetz, Z. anorg. u. allgem. Chem., 271, 6 (1952).
7. F. Hund, U. Peetz, and G. Kottenhahn, Z. anorg. u. allgem. Chem., 278, 184 (1955).
8. F. Hund and U. Peetz, Z. anorg. u. allgem. Chem., 267, 189 (1952).
9. F. Hund and U. Peetz, Z. Elektrochem., 56, Series 3, 223 (1952).
10. W. Rudorff and G. Valet, Z. anorg. u. allgem. Chem., 271, 257 (1953).
11. W. Trzebiatowski and P. Selwood, J. Am. Chem. Soc., 72, 4504 (1950).
12. E. Slowinski and N. Elliott, Acta Cryst., 5, 768 (1952).
13. W. Lambertson and M. Mueller, J. Am. Ceram. Soc., 37, 10 (1954).
14. F. Hund and G. Niessen, Z. Elektrochem., 56, 972 (1952).
15. J. S. Anderson, N. D. Edgington, L. E. J. Roberts, and E. Wait, J. Chem. Soc., 3324 (1954).
16. S. W. Kurnick, J. Chem. Phys. 20, 218 (1952).
17. W. Hartmann, Z. Physik, 102, 709 (1936).
18. K. Hauffe and A. Rahmel, Z. physik. Chem., 1, New Series, 104 (1954).
19. K. Hauffe, Z. physik. Chem., B 48, 124 (1941).

20. W. Meyer, Z. tech. Phys., 14, 126 (1933); also, Z. Physik, 85, 287 (1933).

21. K. T. Perkins, University of Chicago, Metallurgical Laboratory Report CT-1008, October 1943.

22. E. S. Wright and J. T. Waber, unpublished data.

23. J. J. Katz and E. Rabinowitch, "The Chemistry of Uranium," National Nuclear Energy Series, Div. VIII, Vol. 5, p. 238, McGraw-Hill Book Company, New York, 1951.

24. W. E. Lindlief, National Bureau of Standards Report CT-2733, March 1945; see also, M. Mallett, Battelle Memorial Institute Report CC-688, May 1943.

25. S. F. Waber and J. T. Waber, Los Alamos Scientific Laboratory Report LAMS-1841, December 1951.

26. H. Hoxeng and W. Rebol, University of Chicago, Metallurgical Laboratory Report CT-687, Part II, May 1943; CT-753, Part II, June 1943.

27. M. Kolodoney and A. Covert, Los Alamos Scientific Laboratory Report LA-313, June 1945.

28. D. T. Vier, M. L. Schultz, and J. Bigeleisen, J. Opt. Soc. Amer., 38, 811 (1948).

29. R. H. Christ, Columbia University, SAM Laboratories Report A-146, September 1943.

30. J. Aloy, Bull. soc. chim. Paris, 21, Series 3, 613 (1899).

31. T. Wathen, Brown University Report BM-89, May 1943.

32. W. A. Mollison, G. C. English, and F. Nelson, University of Chicago, Metallurgical Laboratory Report CT-3055, June 1945; see also, J. E. Draley and G. C. English, University of Chicago, Metallurgical Laboratory Report CT-1943, July 1944.